Research Article
Vol. 26, No. 13 | 25 Jun 2018 | OPTICS EXPRESS 17009
Optics EXPRESS

Selective variable optical attenuator for visible and mid-Infrared wavelengths

SHENG-PING CHIANG,[1,4] CHUN-TA WANG,[2,4] TING-MAO FENG,[2] CHENG-CHANG LI,[2] HUNG-CHANG JAU,[2] SHANG-YI SU,[2] SHANG-DA YANG,[3] AND TSUNG-HSIEN LIN[2,*]

[1]*Department of Electrical Engineering, National Sun Yat-sen University, Kaohsiung, Taiwan*
[2]*Department of Photonics, National Sun Yat-sen University, Kaohsiung, Taiwan*
[3]*Institute of Photonics Technologies, National Tsing Hua University, Hsinchu 30013, Taiwan*
[4]*Equally contributed to this work*
[*]*jameslin@faculty.nsysu.edu.tw*

Abstract: This work demonstrates a variable optical attenuator (VOA) using dynamic scattering mode (DSM) in ion-doped liquid crystals with negative dielectric anisotropy. The mechanism of attenuation comes from optical scattering, which is generated by the electrically induced instability of undulation of LC textures. Electric fields are applied to switch the initial transparent state of the designed VOA to scattering states, varying the transmittance. The electric field also changes the size of the scattering domain from the LC texture and causes the designed device to exhibit an ultra-broadband selective operation in a visible to mid-IR spectral range. Furthermore, the VOA can selectively block one visible or mid-IR wavelength of light while letting other light pass. Such a VOA has many superior optical switching properties, such as high on/off contrast, insensitivity to polarization, and spectral selectivity; therefore, it has the potential to be used in practical optical systems.

OCIS codes: (160.3710) Liquid crystals; (230.3720) Liquid-crystal devices; (260.3060) Infrared.

References and links

1. R. Baetens, B. P. Jelle, and A. Gustavsen, "Properties, requirements and possibilities of smart windows for dynamic daylight and solar energy control in buildings: A state-of-the-art review," Sol. Energy Mater. Sol. Cells **94**(2), 87–105 (2010).
2. D. K. Yang and S. T. Wu, *Fundamentals of Liquid Crystal Devices* (Wiley, 2006).
3. C. G. Granqvist, "Electrochromics for smart windows: Oxide-based thin films and devices," Thin Solid Films **564**, 1–38 (2014).
4. M. C. Wu, O. Solgaard, and J. E. Ford, "Optical MEMS for lightwave communication," J. Lightwave Technol. **24**(12), 4433–4454 (2006).
5. A. L. Dyer, C. R. G. Grenier, and J. R. Reynolds, "A poly(3,4-alkylenedioxythiophene) electrochromic variable optical attenuator with near-infrared reflectivity tuned independently of the visible region," Adv. Funct. Mater. **17**(9), 1480–1486 (2007).
6. E. Nicolescu, C. Mao, A. Fardad, and M. Escuti, "Polarization-insensitive variable optical attenuator and wavelength blocker using liquid crystal polarization gratings," J. Lightwave Technol. **28**(21), 3121–3127 (2010).
7. H. Ren and S. T. Wu, "Optical switch using a deformable liquid droplet," Opt. Lett. **35**(22), 3826–3828 (2010).
8. Q. Liu, X. M. Zhang, H. Cai, A. B. Yu, and C. Lu, "Retro-axial VOA using parabolic mirror pair," IEEE Photonics Technol. Lett. **19**(9), 692–694 (2007).
9. C. Lee and J. A. Yeh, "Development and evolution of MOEMS technology in variable optical attenuators," J. Micro/Nanolith **7**(2), 021003 (2008).
10. H. W. Ren, S. Xu, Y. F. Liu, and S. T. Wu, "Liquid-based infrared optical switch," Appl. Phys. Lett. **101**(4), 041104 (2012).
11. T. H. Choi, J. W. Kim, and T. H. Yoon, "Fast in-plane switching of negative liquid crystals using crossed patterned electrodes," Jpn. J. Appl. Phys. **53**(8), 081701 (2014).
12. H. Shim, H. K. Lyu, B. Allabergenov, Y. Garbovskiy, A. Glushchenko, and B. Choi, "Enhancement of frequency modulation response time for polymer-dispersed liquid crystal," Liq. Cryst. **5377**, 1–7 (2016).
13. J. Murray, D. Ma, and J. N. Munday, "Electrically controllable light trapping for self-powered switchable solar windows," ACS Photonics **4**(1), 1–7 (2017).
14. G. H. Lee, K. Y. Hwang, J. E. Jang, Y. W. Jin, S. Y. Lee, and J. E. Jung, "Characteristics of color optical shutter with dye-doped polymer network liquid crystal," Opt. Lett. **36**(5), 754–756 (2011).

#330691
Journal © 2018
https://doi.org/10.1364/OE.26.017009
Received 1 May 2018; revised 13 Jun 2018; accepted 14 Jun 2018; published 18 Jun 2018

15. F. Du, Y. Q. Lu, H. W. Ren, S. Gauza, and S. T. Wu, "Polymer-stabilized cholesteric liquid crystal for polarization-independent variable optical attenuator," Jpn. J. Appl. Phys. **43**(10), 7083–7086 (2004).
16. A. Moheghi, H. Nemati, Y. Li, Q. Li, and D. K. Yang, "Bistable salt doped cholesteric liquid crystals light shutter," Opt. Mater. **52**, 219–223 (2016).
17. Y. H. Fan, Y. H. Lin, H. Ren, S. Gauza, and S. T. Wu, "Fast-response and scattering-free polymer network liquid crystals for infrared light modulators," Appl. Phys. Lett. **84**(8), 1233–1235 (2004).
18. M. W. Geis, P. J. Bos, V. Liberman, and M. Rothschild, "Broadband optical switch based on liquid crystal dynamic scattering," Opt. Express **24**(13), 13812–13823 (2016).
19. S. V. Serak, U. Hrozhyk, J. Hwang, N. V. Tabiryan, D. Steeves, and B. R. Kimball, "High contrast switching of transmission due to electrohydrodynamic effect in stacked thin systems of liquid crystals," Appl. Opt. **55**(30), 8506–8512 (2016).
20. E. A. Konshina and D. P. Shcherbinin, "Study of dynamic light scattering in nematic liquid crystal and its optical, electrical and switching characteristics," Liq. Cryst. **45**(2), 292–302 (2018).
21. S. Kai, K. Yamaguchi, and K. Hirakawa, "Observation of flow figures in nematic liquid crystal MBBA," Jpn. J. Appl. Phys. **14**(11), 1653–1658 (1975).
22. B. Guo, Y. Wang, C. Peng, H. Zhang, G. Luo, H. Le, C. Gmachl, D. Sivco, M. Peabody, and A. Cho, "Laser-based mid-infrared reflectance imaging of biological tissues," Opt. Express **12**(1), 208–219 (2004).
23. V. A. Serebryakov, E. V. Boiko, N. N. Petrishchev, and A. V. Yan, "Medical applications of mid-IR lasers. Problems and prospects," J. Opt. Technol. **77**(1), 6–17 (2010).
24. G. Garcia, R. Buonsanti, E. L. Runnerstrom, R. J. Mendelsberg, A. Llordes, A. Anders, T. J. Richardson, and D. J. Milliron, "Dynamically modulating the surface plasmon resonance of doped semiconductor nanocrystals," Nano Lett. **11**(10), 4415–4420 (2011).
25. A. Llordés, G. Garcia, J. Gazquez, and D. J. Milliron, "Tunable near-infrared and visible-light transmittance in nanocrystal-in-glass composites," Nature **500**(7462), 323–326 (2013).

1. Introduction

A variable optical attenuator (VOA) is an essential optical component that can modulate the intensity of light and has many applications in smart windows, the military, and optical telecommunication networks [1–5], which depend on its operating spectra. Various materials, including liquid crystal (LC) materials and electro-chromic materials, as well as electro-wetting and microelectromechanical systems (MEMS), have been proposed to realize VOAs [6–10]. LC-based VOAs are attracting considerable interest owing to their favorable properties, such as an absence of moving-parts, low power consumption, and ease of fabrication. Two common mechanisms of attenuation of light intensity in existing LC-VOAs are based on optical absorption and scattering properties [11–16]. The former normally requires the use of dichroic dyes or polarizers to absorb light. Although such LC-VOAs usually have the lower driving voltages, they are polarization-dependent because of the anisotropic properties of the LC molecules, and they exhibit narrowband operation, which is limited by the absorption spectra of the dichroic dyes or polarizers. In contrast, the latter exhibit polarization-independence and broadband operation (~few hundred nanometers). The most widely used techniques in realizing scattering-type LC-VOAs is to adopt liquid crystal/polymer composites, including polymer-dispersed liquid crystal (PDLC) [12,13], polymer network liquid crystal (PNLC) [14], and polymer-stabilized cholesteric liquid crystal (PSCLC) [15,16]. After phase separation in liquid crystal/polymer composites, polymer networks or LC droplets are generated, depending on the adopted polymer materials, and so optical scattering occurs as a result of the mismatch of the refractive index in the polymer and the LCs. Optical scattering properties, especially scattering wavelengths, depend strongly on the size of network/LC droplets. By properly optimizing the polymer concentration and phase separation conditions, the scattering of light in different wavelength ranges can be enhanced or suppressed. (For example, the VOA can be made transparent in the near-infrared (NIR) region, but scattering in visible region.) [17] In fact, the operating spectrum of such LC-VOAs is fixed because phase separation does not change network/droplet domain sizes. Therefore, most studies have focused on LC-VOAs with a single operating spectrum that covers only visible or NIR regions. Currently, such LC-VOAs with broadband operation that cover multi-spectra are hard to realized.

Another class of scattering-type LC-VOAs that use the dynamic scattering mode (DSM) effect has been reported [18–20]. The DSM effect is attributed to electro-hydrodynamic

(EHD) instability, which is frequently observed when a low-frequency electric field is applied to an LC with a negative dielectric anisotropy ($\Delta\varepsilon < 0$) and a positive conductivity anisotropy ($\Delta\sigma > 0$). Such EHD instability can generate multi-domains of an LC texture with the aid of electric fields, enabling optical scattering. DSM-VOAs have many of the advantages of LC-VOAs that use liquid crystal/polymer composites, including polarization-independence and broadband operation; they also require relatively low driving voltages. Additionally, DSM-VOAs are polymer-free, so the sizes of the domains in the LC texture are unlimited and vary as the electric fields are increased [21]. Their variable domain sizes make a VOA uniquely able to exhibit ultra-broadband operation and spectral selectivity.

This work proposes a polarization-independent LC-VOA that is based on a DSM cell. Such a proposed VOA can operate with an ultra-wide spectrum that covers the visible to the mid-infrared (mid-IR) range. Despite its many possible applications, only a few papers presented an LC-VOA that operates in the mid-IR region. The feasibility of selecting between visible and mid-IR ranges in such a VOA is demonstrated.

2. Experimental section

The mixture that is used to produce the DSM cell comprises 0.1wt% ionic material TBATFB (from Sigma-Aldrich) and a nematic LC DNM-A that exhibits negative dielectric anisotropy (n_e = 1.58, n_o = 1.48, $\Delta\varepsilon$ = −3.3). The ionic material was added to LCs to increase their conductivity. After the mixture thus formed was stirred in the isotropic phase for four hours to ensure homogeneous mixing, it was used to fill an empty cell, which was made of two pieces of sapphire substrate with a thickness of 26 μm. The substrates were pre-coated with conducting indium-tin-oxide (ITO) layers as electrodes and polyimide films to ensure the homogeneous alignment of the LC molecules. Cooling to room temperature formed the DSM cell. The used ITO-coated sapphire substrate was transparent to the entire observed spectrum from visible (transmittance ~90%) to mid-IR (transmittance ~82% at λ = 2.5–5 μm).

In the experiment, the electro-optical performance of the DSM cell in visible and mid-IR regions was evaluated using an intra-cavity optical parametric oscillator-type mid-IR Nd:YVO4 laser (λ = 3μm) and a red He-Ne laser (λ = 632.8 nm) as light sources. Transmission spectra in the visible/near-infrared (NIR) and mid-IR regions were obtained using an optical spectrum analyzer (OSA) (AQ-6315E, ANDO) and a Fourier transform infrared spectroscope (FTIR) (VERTEX 70v, Bruker), respectively. A function generator (33220A, Agilent) connected to an amplifier (A400DI, FLC Electronics) was used to apply electric fields to the DSM cell, and a source meter (Model 2400, Keithley) was employed to measure the electrical current of the DSM cell. All transmission measurements were referenced to the DSM cell in the absence of the electric field to diminish the color dispersion of absorption in ITO layers and sapphire substrates.

3. Results and discussion

The mechanism of the DSM effect is as follows. Before electric field is applied, all LC molecules in the DSM cell are aligned parallel to the substrate and along the rubbing direction. The DSM cell with a single-domain structure is transparent. When an electric field is applied, the electric field forces the LC molecules to align perpendicular to the electric field owing to their negative dielectric anisotropy, while the charge buildup that is induced by positive ions tends to align the LC molecules perpendicular to the substrate. Consequently, the competition between forces generates a shear torque on the molecules and thus causes the generation of a multi-domain structure with periodic patterns, comprising so-called “Williams domains.” When an electric field increases to a critical strength, the material produces a turbulence, as the pattern of the multi-domain structure begins to change from regular to random, causing the device to scatter light. This state is called the DSM state. According to Mie scattering theory, optical scattering usually typically takes place when the size of the scattering particles is comparable to the wavelength of the light. This result reveals that the optical scattering wavelength of the DSM cell is determined by the domain sizes of the LC texture.

An ultra-broadband VOA that is based on the DSM cell in which domain sizes are changed through the application of electric fields, is designed. Figure 1 schematically depicts its operational principles. When biases are applied below a critical electric field, the DSM cell is transparent across the entire spectrum. When an electric field that slightly exceeds the critical field is applied, the DSM state begins to scatter light whose wavelength is relatively longer. As the field increases, the size of the domains in the LC texture gradually declines, so the optical scattering wavelength is reduced [21]. Long and short wavelengths refer to mid-IR and visible light, respectively. Therefore, the multi-spectral operation of VOA can be realized on the basis of the electrical tuning of the domain sizes of the LC texture in the DSM cell.

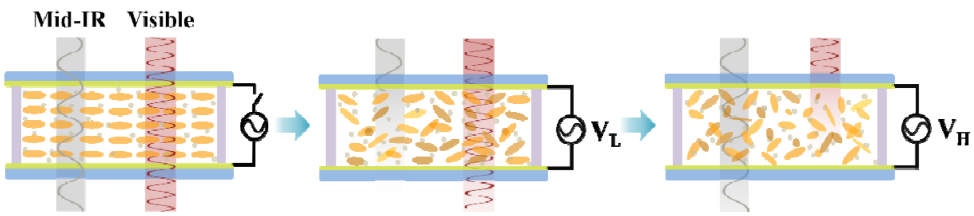

Fig. 1. Operation of proposed VOA based on DSM cell under the influence of an electric field.

To verify the above design, the dependence of the transmittance of the DSM cell on the electrical field was firstly measured using a 632.8 nm He-Ne laser and a 3 μm Nd:YVO4 laser.

Both lasers emit linear polarized beam and the direction of polarization is along the direction parallel the long axes of the LC molecules. The transmittance of the DSM cell is sensitive to the detection distance and the reception angle of the detector. Typically, the farther detection distance and the narrower reception angle can effectively enhance contrast of DSM cell due to the lower transmittance received in the off-state. In the following measurements, the distance between the DSM cell and a photodiode was ~15 cm, and the half cone angle of received radiation at the detector was set to be 0.19°. In addition, an applied electric field (square-wave) with a frequency of 240 Hz is used due to the superior performance of on/off contrast relative to fields with others frequencies (not shown here). As expected, a significant difference between the two transmittance-voltage (T-V) curves of 632.8 nm and 3 μm lasers is observed, as depicted in Fig. 2(a). In an electric field that is weaker than the critical field of 0.7 V/μm, the DSM cell is fully transparent to both 632.8 nm and 3 μm lasers. As the electric fields below 0.92 V/μm, the transmittance to both lasers begins to be reduced by optical scattering. The fact that the transmittance to the 632.8 nm laser varies much less than the transmittance to the 3 μm laser reveals that the domain size of the LC texture is closer to the wavelength of 3 μm than to that of 632.8 nm. In an applied electric field is increased above 1.54 V/μm, the domain size of the LC texture is gradually reduced, causing a blue-shift in the optical scattering wavelengths; thus, the transmittance to the 3 μm laser ceases to decay and begins to rise instead, while the transmittance of the 632.8 nm laser gradually decreases and becomes saturated. Both curves are consistent with the hypothesis that variation of the domain sizes in the LC texture shifts the scattering wavelength of the DSM cell. Further evidence to support this hypothesis is provided by the microscopic images of the DSM cell that were taken using a polarizing optical microscope with crossed polarizers and shown in Fig. 2(c). The error bars in Fig. 2(a) were derived by measuring different DSM cells. The wider range of error bars, especially in the sharp transition region, is mainly associated with a slight difference in cell gap among these DSM cells. Moreover, the polarization-independency of the DSM cell was examined. Figure 2(b) plots the V-T curves of the DSM cell with the 3 μm laser as a probe. The parallel- and perpendicular- curves refer to the probe beam whose direction of polarization is parallel and perpendicular to the long axes of the LC molecules, respectively. The results show that no obvious difference between both curves was found and indicates that the designed DSM cell is polarization insensitive despite of the homogeneous alignment of LC molecules. Figure 2(d) displays photographs of the DSM cell in at different electric fields. Initially, the DSM cell is transparent to visible light; it then gradually switches to the scattering state as the electric field is increased. Under a bias of 1.54 V/μm, the DSM cell entirely becomes opaque, so the image behind the DSM cell is totally invisible. Despite the fact that the LC domain structure in DSM state remains in a dynamic state, for a given bias the corresponding domain size of the LC texture is gradually fixed, and thus the transmittance of the DSM cell becomes stable. The response time required for obtaining the stable transmittance is around a few hundred milliseconds to few seconds range, depending on the applied electric fields. The electrical current through the DSM cell is only few microamperes, and so such a low current has less influence on the optical properties of the DSM cell.

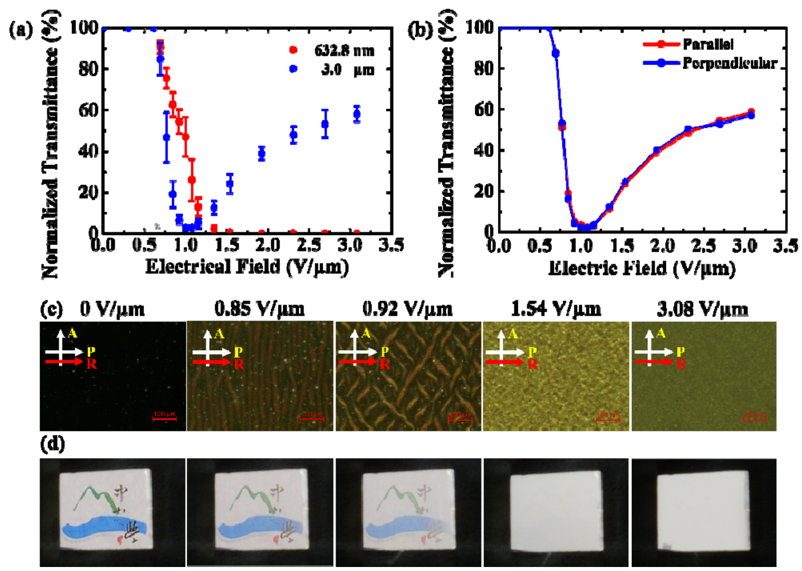

Fig. 2. Electric field-dependent transmittance of designed device (a) at λ = 632.8 nm and 3 μm, and (b) at λ = 3 μm with different direction of polarization. (c) Micro-graphs and (d) photographs of designed device at different fields.

To understand further the electro-optical behavior of the DSM cell in each part of the spectrum, transmission spectra in the visible, near-IR, and mid-IR regions were measured with various electrical fields. The corresponding spectral windows are 0.45–0.75 μm, 0.75–1.7 μm, and 2.5–3.2 μm. As can be seen in Fig. 3, the transmittance of the designed device can be reversibly switched by varying the field strength. In spite of the fact that different biases are required to obtain the same transmittance, the transmittance can be varied almost from 100 to 0%, revealing that the DSM cell indeed exhibits broadband operation from visible to mid-IR regions. The minimum transmittance in the mid-IR and visible/NIR regions can be achieved by applying electric fields of 1.54 and 1.15 V/μm, respectively. The difference in the electric field strengths between regions is attributed to the correlation between the domain size in the LC texture and the wavelength of the incident light. Moreover, the attenuation behavior of the DSM cell in both visible and mid-IR regions is less sensitive to wavelength than is that in the NIR region. Some noise appears in the mid-IR spectra is associated with atmospheric measurement environment of FTIR.

The consequence that the DSM cell exhibits optical scattering in a manner determine by the domain size in the LC texture, which can be controlled by external electrical fields, supports a remarkable optical switching function and operational spectral selectivity between visible and mid-IR regions (and thus the independent modulation of visible and mid-IR light). For example, at biases between 0.92 and 1.15 V/μm, the DSM cell blocks mid-IR light but allows visible light to pass with a tunable transmittance from ~55 to 15%. When operated at electrical fields between 1.54 and 3.08 V/μm, the DSM cell scatters the visible light but is partially transparent to mid-IR light, the transmittance to which can be tuned from ~20 to 60%, as shown in Fig. 4. Such an operational spectral selectivity between visible and mid-IR regions may be useful for particular applications, such as mid-IR image sensors or mid-IR military lasers [22,23]. In these applications, a visible light source is often required to capture visible images or to image targets; therefore, a VOA that can selectively block visible and mid-IR light is highly desired. Until now, only a few investigations reported on spectral selectivity between visible and NIR regions for an electrochromic material or a nanocrystal-in-glass composite [24,25]. To the best of our knowledge, spectral selectivity between visible light and mid-IR light has not yet been demonstrated in VOAs.

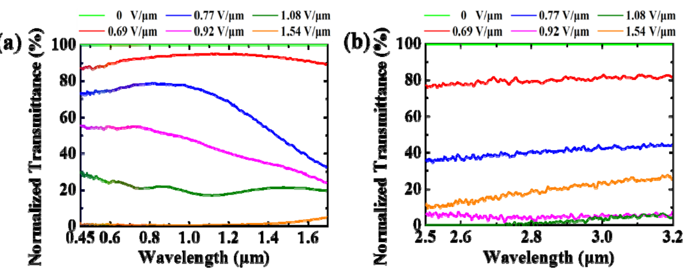

Fig. 3. Transmission spectra of proposed device at several bias fields in (a) visible/NIR regions and (b) mid-IR regions.

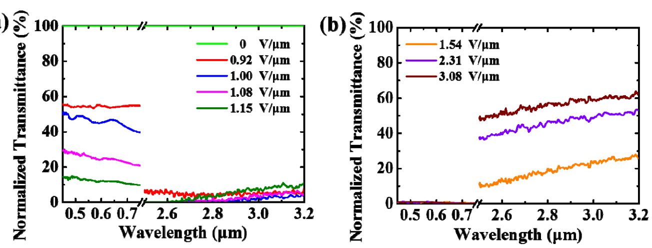

Fig. 4. Spectral selectivity between visible and mid-IR regions in bias fields (a) between 0 and 1.15 V/μm and (b) between 1.54 and 3.08 V/μm.

4. Conclusion

This work demonstrates a VOA that is based on the DSM effect in a LC cell. The electrically induced DSM effect can give rise to turbulence in the LC texture, causing optical scattering and realizing the attenuation of light. The application of an electrical field changes the sizes of the scattering domains in the LC texture and thereby shifts the optical scattering wavelength, enabling the designed device to be operated in an ultra-wide spectrum that covers the visible, NIR, and mid-IR regions. For each spectral range, the attenuation strength can be reversibly switched by varying the field strength. A novel optical switching functionality and operational spectral selection of the designed VOA are realized. It can block either visible light or mid-IR light while transmitting the other at particular biases. This designed VOA exhibits polarization-independence, ultra-broadband operation, and spectral selectivity, and so has great potential for many applications, and especially for use in mid-IR devices.

Funding

Ministry of Science and Technology of Taiwan (MOST) (106-2112-M-110-003-MY3, 104-2218-E-110-008-MY3, 104-2112-M-007-012-MY3).